Capillary assisted deposition of carbon nanotube film for strain sensing

Zida Li, Xufeng Xue, Feng Lin, Yize Wang, Kevin Ward, and Jianping Fu

Citation: Appl. Phys. Lett. **111**, 173105 (2017);
View online: https://doi.org/10.1063/1.5001754
View Table of Contents: http://aip.scitation.org/toc/apl/111/17
Published by the American Institute of Physics

Capillary assisted deposition of carbon nanotube film for strain sensing

Zida Li,[1] Xufeng Xue,[1] Feng Lin,[1] Yize Wang,[1] Kevin Ward,[2,3] and Jianping Fu[1,3,4,5,a)]
[1]*Department of Mechanical Engineering, University of Michigan, Ann Arbor, Michigan 48109, USA*
[2]*Department of Emergency Medicine, University of Michigan, Ann Arbor, Michigan 48109, USA*
[3]*Michigan Center for Integrative Research in Critical Care, University of Michigan, Ann Arbor, Michigan 48109, USA*
[4]*Department of Biomedical Engineering, University of Michigan, Ann Arbor, Michigan 48109, USA*
[5]*Department of Cell and Developmental Biology, University of Michigan Medical School, Ann Arbor, Michigan 48109, USA*

(Received 26 August 2017; accepted 16 October 2017; published online 26 October 2017)

Advances in stretchable electronics offer the possibility of developing skin-like motion sensors. Carbon nanotubes (CNTs), owing to their superior electrical properties, have great potential for applications in such sensors. In this paper, we report a method for deposition and patterning of CNTs on soft, elastic polydimethylsiloxane (PDMS) substrates using capillary action. Micropillar arrays were generated on PDMS surfaces before treatment with plasma to render them hydrophilic. Capillary force enabled by the micropillar array spreads CNT solution evenly on PDMS surfaces. Solvent evaporation leaves a uniform deposition and patterning of CNTs on PDMS surfaces. We studied the effect of the CNT concentration and micropillar gap size on CNT coating uniformity, film conductivity, and piezoresistivity. Leveraging the piezoresistivity of deposited CNT films, we further designed and characterized a device for the contraction force measurement. Our capillary assisted deposition method of CNT films showed great application potential in fabrication of flexible CNT thin films for strain sensing. *Published by AIP Publishing.*
https://doi.org/10.1063/1.5001754

Conventional electronics, which is based on printed circuit boards and silicon wafers, is inherently rigid and lacks flexibility and stretchability. While the mainstream research in conventional electronics has been focused on developing faster and smaller units on planar surfaces, there is an emerging development of stretchable devices for applications such as wearable electronic devices and health monitoring sensors. The curvy nature of biological objects requires electronics to be stretchable to ensure conformable contact. Such a need of stretchability led to the emerging field of stretchable electronics.[1]

Two major concepts have been successfully adopted for developments of stretchable electronics. One is to make specially designed thin structures before transferring them onto stretchable substrates such as polymers, forming either wavy or island-bridge structures.[2] Such a design minimizes strain in the brittle silicon or metal materials and allows bending and stretching. Successful applications in skin sensors,[3] cardiac monitoring,[4] etc., have been reported using this approach. The other concept applies new functional materials, oftentimes combined with polymers, to make elastic conductors. Among these new materials, carbon nanotubes (CNTs) are one of the most commonly used materials given their exceptional electronic properties. Besides their diverse semiconducting properties as a result of tunable chirality,[5] CNTs have great electron mobility and thus excellent conductivity. In addition, although single CNTs have high Young's modulus, the carbon nanotube network shows good stretchability.[6]

Direct growth based on chemical vapor deposition (CVD) has been the most common fabrication method of CNT films.[7] Such methods fabricate CNT films with good conductivity; however, they generally require high temperature, which is not compatible with most polymer substrates. Alternatively, solution-based deposition methods are more friendly to polymer substrates although the conductivity of CNT films is compromised compared to CVD.[7]

Many methods based on solution deposition have been proposed, including dip coating,[8] contact printing,[9] inkjet printing,[10] solution precipitation,[11] and spray coating.[12] However, these methods are either complicated to implement or not capable of generating desired patterns on substrates. In this paper, we report a simple yet convenient method to generate patterns of piezoresistive CNT films on the surfaces of elastic polydimethylsiloxane (PDMS). In particular, micropillar arrays were fabricated on the PDMS surface before these surfaces were rendered hydrophilic. After CNT solutions were dispensed onto the PDMS surface, capillary action drove the solution evenly onto the surface area covered with micropillars. Water evaporation left a uniform film of CNTs deposited on the PDMS surface, with the shape of the envelope of the micropillar array. The effects of the CNT concentration and micropillar gap size on coating uniformity, conductivity, and piezoresistivity of CNT films were studied. Leveraging the piezoresistivity of deposited CNT films, we further designed and characterized a contraction force measurement device that could be useful for different biomedical and biological applications. Our capillary assisted deposition method of CNT films shows the potential of being applied in fabrication of flexible CNT thin films for strain sensing,[6,13] which can be used in motion sensors in stretchable electronics and in contraction sensors in biomedical devices.

The PDMS micropillar array had two major effects on deposition of CNT films on PDMS surfaces. First, when

a)Author to whom correspondence should be addressed: jpfu@umich.edu

CNT solution was dispensed on PDMS surfaces, capillary force facilitated CNT solution spreading and confined CNT solution in the area with micropillars. Such a confining effect provided an effective way to pattern the CNT film. Second, the micropillar array restrained the coffee ring effect. The coffee ring effect originates from the compensating flow that keeps the contact line fixed,[14] making particle deposition concentrated on the liquid perimeter, as shown in Fig. 1(a). The micropillar array provided multiple evenly distributed contact lines, suppressing the coffee ring effect and thus leading to a more uniform CNT deposition compared to PDMS surfaces without micropillar arrays [Figs. 1(b) and S1].

The CNT film deposited on PDMS surfaces with micropillar arrays also showed good uniformity at the microscale, as demonstrated by phase-contrast and scanning electron microscope images [Fig. 1(c)]. Compared to raw CNTs, CNTs were broken up into smaller bundles in the stock solution by sonication during sample preparation (see supplementary material). For example, at a concentration of 0.808 mg/ml, CNTs appeared as individual fibers in contact with neighboring fibers, forming a connected network. The thickness of deposited CNT films was about 40 nm, as measured by atomic force microscopy [Fig. S2(a), supplementary material].

We investigated the conductivity of deposited CNT films and its dependence on the CNT concentration. With a CNT concentration of 1.616 mg/ml, the conductivity of the CNT film was $11.16 \pm 1.23\ \mu S \cdot sq^{-1}$. As the CNT concentration became lower, CNT film conductivity decreased exponentially [Fig. 1(d)], consistent with the percolation theory studying through pathways of randomly connected clusters in a random graph.[15,16] Specifically, our data agreed well with predictions made by the percolation theory that simulates each CNT fiber as a conducting stick (CS), overlapping with other CNTs and forming a connected network. The percolation theory predicts that the conductivity of a two-dimensional film depends on the density of particles following

$$\sigma \propto (N - N_c)^{\alpha}, \tag{1}$$

where σ is the conductivity, N is the CS density, N_c is the critical CS density above which percolation happens, and the exponent $\alpha = 1.33$.[15] The CS density scales linearly with the CNT concentration, which gives

$$\sigma \propto (\rho - \rho_c)^{\alpha}, \tag{2}$$

where ρ is the CNT concentration and ρ_c is the critical CNT concentration. The fitting of the CNT sheet conductance experimental data using Eq. (2) gave a ρ_c of 0.308 mg/ml and an exponent α of 1.61, which was close to the theoretical value of 1.33 but somewhat greater. This discrepancy potentially resulted from the fact that CNT films deposited on PDMS surfaces were not perfectly two-dimensional, which was particularly evident at higher CNT concentrations [Fig. 1(c)]. The percolation theory predicts the critical exponent α of 1.94 for three-dimensional, randomly connected clusters.[15]

Micropillar gap size is a major geometric parameter that affects CNT film deposition on PDMS surfaces since it is directly related to the contact line number, affecting the extent of the coffee ring effect and thus CNT film deposition.[14] We thus sought to determine the micropillar gap size that could result in optimal CNT film deposition. Here, we define CNT film surface coverage as the ratio of areas covered with the CNT film to the total area of the channel bottom. As shown in Figs. 2(a) and 2(b), micropillar arrays with a gap size of 80 μm and 150 μm had a high surface coverage of $79.3 \pm 1.0\%$ and $76.4 \pm 2.4\%$ by CNT films, respectively. When the micropillar gap size became smaller or larger out of this range, deposited CNT films became less uniform with less surface areas covered by deposited CNT films. For example, for micropillar gap sizes of 40 μm and 200 μm, the CNT film coverage was $52.1 \pm 7.0\%$ and $58.7 \pm 2.2\%$,

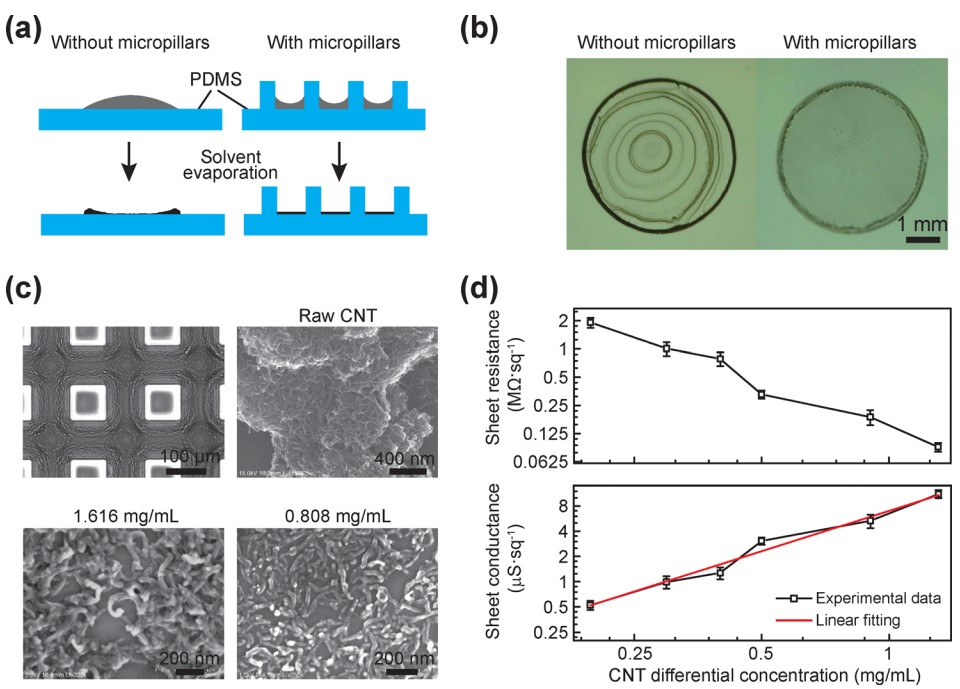

FIG. 1. (a) Schematic showing capillary-assisted deposition of CNT films on PDMS surfaces. (b) Photograph showing CNTs deposited on PDMS surfaces without (left) or with (right) micropatterned structures. (c) Upper left: Phase-contrast image showing the CNT film (1.616 mg/ml) deposited on a PDMS surface with a patterned regular array of square shaped pillars. Other SEM images show unprocessed CNT materials and CNT films with different concentrations deposited on PDMS surfaces as indicated. (d) Sheet resistance (top) and conductance (bottom) as a function of the CNT differential concentration as defined in Eq. (1).

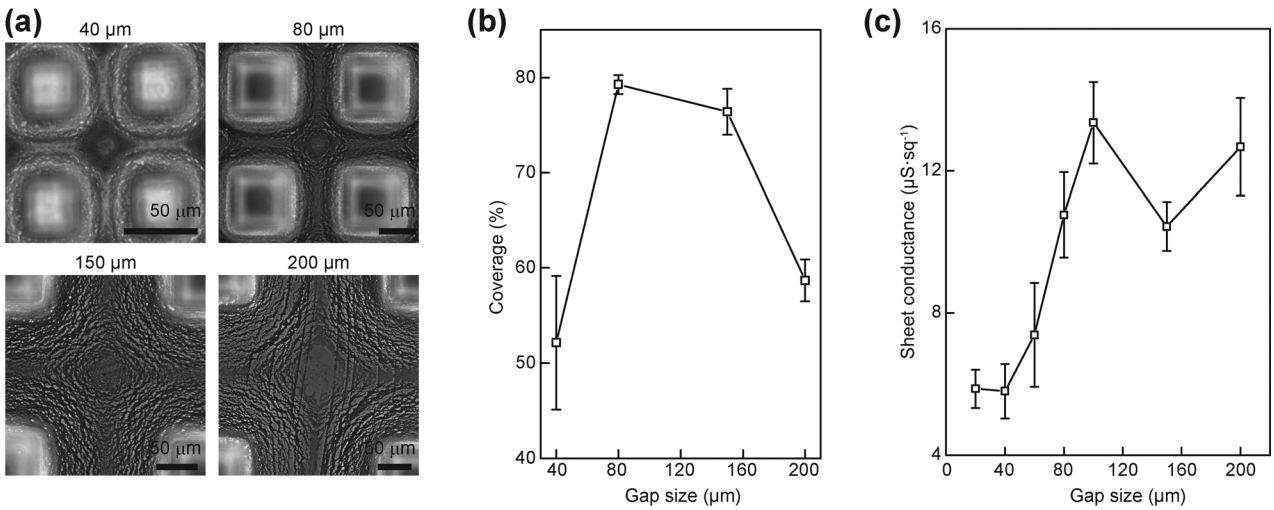

FIG. 2. Effect of pillar gap size on coating uniformity and conductivity of CNT films. (a) Micrographs of CNT films deposited on PDMS surfaces with micropillar arrays with different gap sizes as indicated. (b) and (c) Coverage (b) and sheet conductance (c) of CNT films deposited on PDMS surfaces as a function of micropillar gap size.

respectively. The biphasic effect of micropillar gap size on CNT film coverage was possibly due to multifaceted effects of micropillars on CNT film deposition. The coffee ring effect predicts that solute deposition tends to concentrate around the contact line. As a micropillar array with a smaller gap size has closer contact lines, CNT deposition is supposedly more uniform. However, due to capillary action, CNT solution tends to climb up micropillars and form meniscus, which inevitably results in heightened CNT deposition close to pillar side walls. Thus, the micropillar array with 40 μm gap size had more contacts between CNT solution and pillar walls and thus more meniscus, which potentially led to less uniform CNT deposition on PDMS surfaces.

The sheet conductance of CNT films showed a different dependence on micropillar gap size compared to CNT film coverage [Fig. 2(c)]. When the micropillar gap size was less than 80 μm, similar to CNT film coverage, the sheet conductance was reduced. For example, the sheet conductance of the CNT film with micropillars with 40 μm gap size (5.80 ± 0.77 μS·sq^{-1}) was about half of that of the CNT film with micropillars with 80 μm gap size (10.76 ± 1.20 μS·sq^{-1}). However, when the micropillar gap was greater than 80 μm, unlike CNT film coverage, the CNT sheet conductance remained roughly unchanged around 12 μS·sq^{-1}. Specifically, when the micropillar gap size increased from 80 μm to 200 μm, while the CNT film coverage reduced from $79.3 \pm 1.0\%$ to $58.7 \pm 2.2\%$, the sheet conductance became 12.68 ± 1.38 μS·sq^{-1}, not significantly different from 10.76 ± 1.20 μS·sq^{-1} at 80 μm gap size ($p > 0.05$). This was likely because at 200 μm, even though CNTs showed more aggregation and the CNT film coverage was reduced, CNT fibers were still connected [Fig. 2(a)], and thus, the CNT sheet conductance was not significantly affected. In contrast, with 40 μm micropillar gap size, CNT fibers formed discrete islands, rendering the whole CNT film less conductive.

To explore the potential use of deposited CNT films for strain sensing, we specifically measured the electromechanical properties of CNT films deposited at different concentrations including their gauge factors. We fabricated CNT films in dog-bone shapes [Fig. S2(b), supplementary material] and applied uniaxial stretch along the axial direction of the bone shape while simultaneously monitoring electrical resistance changes in deposited CNT films. As shown in Fig. 3, when the CNT concentrations were 0.808 mg/ml and 1.212 mg/ml, the gauge factor of deposited CNT films increased with applied strain, consistent with previous reports.[17] For example, for a CNT concentration of 1.212 mg/ml, the gauge factor of deposited CNT films was 34.7 and 213.6 with a strain of 0.01 and 0.058, respectively [Fig. 3(b)]. However, when the CNT concentration was increased to 1.616 mg/ml, the relative resistance change in deposited CNT films appeared

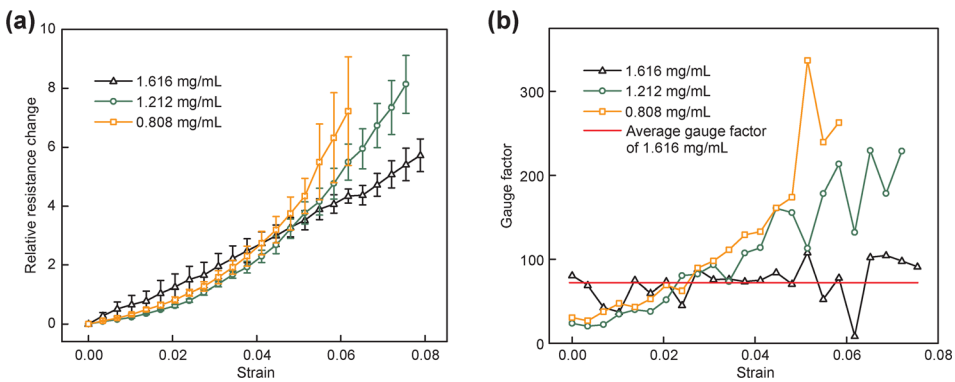

FIG. 3. Relative resistance change (a) and the corresponding gauge factor (b) of CNT films at different CNT concentrations as a function of strain.

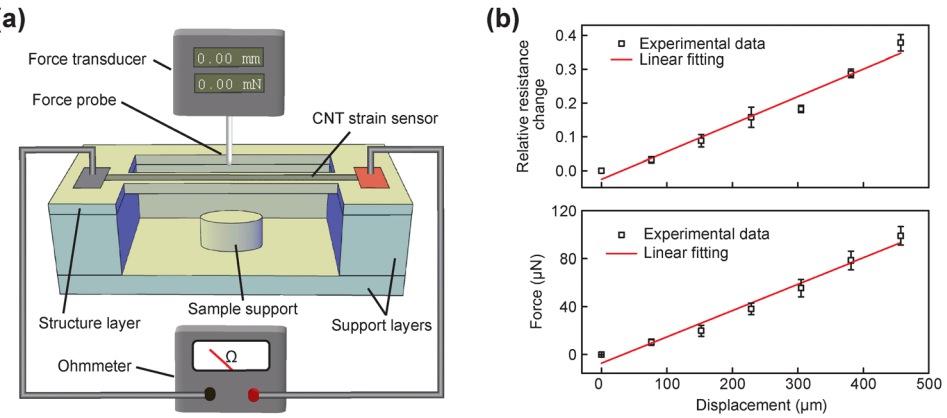

FIG. 4. Application of piezoresistive CNT films for strain sensing. (a) Schematic showing the design of a strain sensing device and its characterization using a probe force transducer. (b) Relative resistance change and required probe force as a function of PDMS beam displacement at the beam center.

linearly increasing with applied strain [$R^2 = 0.99$, data not shown; Fig. 3(a)], leading to a relatively constant overall gauge factor of about 71.8 [Fig. 3(b)]. The linear dependence between the relative resistance change and applied strain at this CNT concentration showed the potential of the CNT films for straining sensing applications.

To demonstrate the utility of piezoresistive CNT films for strain sensing in different biological and biomedical applications, such as blood clot retraction force[18] and cardiac tissue contraction force,[19] we designed a device for the measurement of contraction forces. As shown in Fig. 4(a), this device incorporated a thin PDMS beam as a force sensor, suspended on an acrylic block. A protrusion was designed in the acrylic block for holding and localizing testing samples. The PDMS beam incorporated a micropillar array on its top surface, and a piezoresistive CNT film was deposited on the PDMS beam to render the beam as a strain gauge. To characterize the piezoresistive CNT film for strain sensing, we applied a digital multimeter and a force transducer, which was mounted on a translation stage, to obtain changes in the electrical resistance, applied force, and displacement of the beam center simultaneously. As shown in Fig. 4(b), as the displacement of the beam center increased, the electrical resistance of the CNT strain sensor and applied force increased correspondingly. The ratio of relative resistance change to beam displacement was about $0.8\,\mathrm{mm}^{-1}$, and the spring constant of the beam was about $0.22\,\mathrm{N\cdot m}^{-1}$. Thus, the measurement sensitivity was about 275 μN (per unit change in the relative resistance), which provides a measurement resolution of 0.275 μN if the accuracy of the resistance measurement is 0.1%. Such resolution is capable for measuring cardiac tissue contraction force in the range of 0–10 μN (Ref. 19) and clot contraction force in the range of 0–40 μN.[18]

Carbon nanotubes, as emerging smart functional nanomaterials, have unique electrical properties, rendering them very promising for applications in stretchable electronics. In this work, we report a simple but convenient method for uniform deposition of thin CNT films as strain sensing functional materials on flat PDMS surfaces by fabricating micropillar arrays on the PDMS surfaces and rendering the surfaces hydrophilic through plasma treatments. Owing to capillary forces, CNT solutions dispensed on PDMS surfaces would cover the surfaces uniformly with the shape of the micropillar array. Importantly, the micropillar array would suppress the coffee ring effect to ensure uniform CNT coating on the PDMS surfaces after water evaporation. We studied different parameters that could affect the quality of CNT film deposition, including CNT concentration and micropillar gap size. By studying the piezoresistivity of CNT films and integrating deposited CNT films into a strain sensing device for the tissue contraction measurement, we showed that the CNT film holds great potentials in applications of strain sensing.

Compared to other solution-based CNT deposition processes such as spray coating, our method does not require stencil for patterning, and thus, it is more suitable in applications where CNT patterning is desirable. Our method is also compatible with most soft-lithography based fabrication processes, making it easily applicable to other research laboratories. We believe that this method will find applications in strain sensing in stretchable electronics and contraction force measurements in biomedical researches.

See supplementary material for experimental methods and supplementary figures.

The authors acknowledge financial support from the National Science Foundation (CMMI 1536087), the Michigan Translational Research and Commercialization for Life Sciences Program (MTRAC), and the U-M Coulter Translational Research Partnership Program. The authors thank Professor Xiaogan Liang and Da Li for assistance with SEM imaging. The Lurie Nanofabrication Facility at the University of Michigan, a member of the National Nanotechnology Infrastructure Network (NNIN) funded by the National Science Foundation, is acknowledged for its support in microfabrication.

[1]J. A. Rogers, T. Someya, and Y. Huang, Science **327**(5973), 1603 (2010).
[2]D.-H. Kim, J.-H. Ahn, W. M. Choi, H.-S. Kim, T.-H. Kim, J. Song, Y. Y. Huang, L. Zhuangjian, L. Chun, and J. A. Rogers, Science **320**(5875), 507 (2008); J. Song, X. Feng, and Y. Huang, Nat. Sci. Rev. **3**(1), 128 (2016).
[3]D.-H. Kim, N. Lu, R. Ma, Y.-S. Kim, R.-H. Kim, S. Wang, J. Wu, S. M. Won, H. Tao, and A. Islam, Science **333**(6044), 838 (2011).
[4]D.-H. Kim, N. Lu, R. Ghaffari, Y.-S. Kim, S. P. Lee, L. Xu, J. Wu, R.-H. Kim, J. Song, and Z. Liu, Nat. Mater. **10**(4), 316 (2011).
[5]X. Liang, *Nanotube Superfiber Materials: Changing Engineering Design* (William Andrew, 2014), Vol. 1, p. 2.
[6]D. J. Lipomi, M. Vosgueritchian, B. C. K. Tee, S. L. Hellstrom, J. A. Lee, C. H. Fox, and Z. Bao, Nat. Nanotechnol. **6**(12), 788 (2011).
[7]L. Hu, D. S. Hecht, and G. Gruner, Chem. Rev. **110**(10), 5790 (2010).
[8]M. H. Andrew Ng, L. T. Hartadi, H. Tan, and C. H. Patrick Poa, Nanotechnology **19**(20), 205703 (2008).
[9]Y. Zhou, L. Hu, and G. Grüner, Appl. Phys. Lett. **88**(12), 123109 (2006).

[10]R. P. Tortorich and J.-W. Choi, Nanomaterials **3**(3), 453 (2013).
[11]M. A. Meitl, Y. Zhou, A. Gaur, S. Jeon, M. L. Usrey, M. S. Strano, and J. A. Rogers, Nano Lett. **4**(9), 1643 (2004).
[12]E. Artukovic, M. Kaempgen, D. S. Hecht, S. Roth, and G. Grüner, Nano Lett. **5**(4), 757 (2005).
[13]T. Yamada, Y. Hayamizu, Y. Yamamoto, Y. Yomogida, A. Izadi-Najafabadi, D. N. Futaba, and K. Hata, Nat. Nanotechnol. **6**(5), 296 (2011).
[14]R. D. Deegan, O. Bakajin, T. F. Dupont, and G. Huber, Nature **389**(6653), 827 (1997).
[15]L. Hu, D. S. Hecht, and G. Grüner, Nano Lett. **4**(12), 2513 (2004).
[16]G. E. Pike and C. H. Seager, Phys. Rev. B **10**(4), 1421 (1974).
[17]Y. Li, W. Wang, K. Liao, C. Hu, Z. Huang, and Q. Feng, Chin. Sci. Bull. **48**(2), 125 (2003).
[18]Z. Li, X. Li, B. McCracken, Y. Shao, K. Ward, and J. Fu, Small **12**(29), 3926 (2016).
[19]W. R. Legant, A. Pathak, M. T. Yang, V. S. Deshpande, R. M. McMeeking, and C. S. Chen, Proc. Natl. Acad. Sci. U.S.A. **106**(25), 10097 (2009).